Development of an autonomous experimental system to identify blisk mistuning

S. Denis [1], S. Hoffait [1], J. Ligot [1], M. Lengele [2], P. Mahy [2], J. de Cazenove [3], J.C. Golinval [4]
[1] V2i,
Av. du Pré Aily 25, 4031 Liège, Belgium

[2] MachineSight,
Rue de la Croix Bande 15, 6900 Marche-en-Famenne, Belgium

[3] Cenaero,
Rue des Frères Wright 29, 6041 Charleroi, Belgium

[4] University of Liège, Aerospace and Mechanical Engineering Department
Allée de la Decouverte 9 (B52/3), 4000 Liège, Belgium

Abstract
The one-piece assembly of bladed disks, named blade integrated disks (blisks), leads to more severe mistuning effects and reduced damping. An accurate mistuning identification methodology is thus necessary for the manufacturers to avoid potential engine failure. This paper proposes a complete autonomous system to identify mistuning in the shortest possible time, with reduced human interventions and with improved accuracy. The Inverse Component Mode Mistuning method is implemented, and the mistuning pattern is immediately determined after the experimental measurements are completed. For this purpose, the blisk is fixed on an electrodynamic shaker and the vibration measurements are performed thanks to an infrared Laser Doppler Vibrometer attached to a robotic arm. The use of a robotic measurement system offers multiple possibilities unthinkable when performed manually: 3D measurements are achievable, the positioning is made very accurate and reproducible, and many points can be measured rapidly and without human operation. A comparative study of the experimental measurements made possible with the test rig proposed is carried out.

1 Introduction

Efficient machining of blisk, also known as IBR (Integrally Bladed Rotor), is a focal point to ensure large production volumes for aircraft engines. Blisk manufacturing and assembly by friction welding is a labor-intensive process demanding high complexity and precision. The main deviations in the produced blisks appear due to (1) kinematic errors in the machine during 5-axis operations, (2) elastic deformation of the blade during the cutting process due to its low rigidity and (3) elastic deformation of the tooling during metal cutting [1]. Post manufacturing processes are thus essential to control and validate the product.

One of the fundamental issues of blisk is mistuning, resulting from small blade to blade variations of structural or geometrical properties. The resonant amplitudes of the structure are very sensitive to small mistuning and can cause important damage to the structure in operation. Quantifying mistuning at the end of the blisks production line is thus primordial for the industry to validate quality standards before integrating the blisk to the engine.

This paper proposes an automated and autonomous mistuning identification system dedicated to blisks. The mistuning identification methodology proposed is firstly presented. Then, the automated experimental test rig and the associated calibration process are described. The complete methodology is then tested on an industrial blisk and a validation procedure is carried out considering a mistuning pattern measured thanks to a more intrusive methodology and additional masses on some blades. A sensitivity study on the experimental measurements to improve the mistuning identification is conducted. 3D vibrational measurements are performed and the gain in accuracy in the identified mistuning pattern is discussed.

2 State of the art

Overall, the mistuning identification of blisks is studied through experimental and numerical approaches. Experimental approaches such as adding masses on all the blades except the one currently tested have shown to give accurate results and are quite easy to perform, as presented by Zhou *et al.* [2]. Nonetheless, these methods require a lot of human intervention, which is error prone and too costly to be profitable. Other numerically oriented mistuning identification techniques such as lumped parameter models [3], high fidelity Finite Element Model (FEM) [4] or Reduced Order Modelling (ROM) [5–8] have been proposed by numerous authors. These approaches are the most efficient and accurate. The proposed mistuning identification system relies on a ROM technique, the Inverse Component Mode Mistuning (ICMM) method specifically.

The Component Mode Mistuning identification method was proposed by Lim *et al.* [9]. This approach requires input data including a complete FEM of the tuned structure and experimental measurements of the actual blisk. Nyssen *et al.* [10, 11] used this method in its inverse form considering only the stiffness mistuning to identify the mistuning of an academic blisk. The paper validates the approach using experimental measurements and known mistuning patterns. Holland *et al.* [12] and Pitchot *et al.* [13] have developed a mistuning identification process using the ICMM method based on traveling wave excitation systems. This allows the prediction of the mistuning patterns during engine operations. The main disadvantage lies in the calibration procedure of the traveling wave excitation systems.

Although mistuning identification techniques have been proposed in recent years, most of them have been used and validated only on academic blisks [10, 12]. Compared to these simple structures, the industrial applications present more challenges due to the complex geometry and to the mass of the drum, which is much more important. Besides, most of the available methodologies require intensive human intervention to perform experimental measurements. This paper proposes an automated and autonomous test rig to identify mistuning on industrial blisks.

3 General methodology

3.1 Identification procedure (ICMM)

The Component Mode Mistuning method proposed by Lim et al. [9] is used in this paper in its inverse form. This Reduced Order Model focuses on mistuning modeled as blades eigenfrequencies variations. A FEM of the whole tuned blisk and the actual blisk experimental modal analysis that represents the mistuned properties of the blisk are used to identify the mistuning of the structure through the Inverse Component Mode Mistuning (ICMM), as illustrated in Fig. 1. The ICMM provides results directly when a proper modal identification of the blisk is performed. This limits the human intervention in the process and makes the whole system almost entirely automatable.

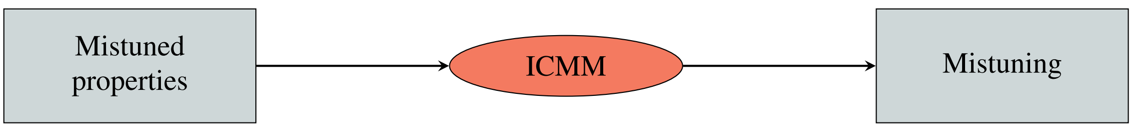

Figure 1: ICMM principle [10]

The identification method for the mistuning patterns is based on the following equation [10]

$$\sum_{n=1}^{N} \mathbf{Q}_n^T \,\mathrm{diag}_{r\in R}\left(\lambda_{n,r}^E\right) \mathbf{Q}_n \mathbf{p} = \frac{1}{(1+i\gamma)} \left[\mathbf{F} + \omega^2 \mathbf{I}\mathbf{p} - (1+i\gamma)\mathbf{\Lambda_0}\mathbf{p}\right], \tag{1}$$

where the parameters are imported from a numerical model of the tuned structure and experimental measurements on the actual blisk, and $\lambda_{n,r}^E$ is the eigenvalue deviation of the r^{th} cantilever blade mode of blade n, allowing deriving the mistuning patterns to be identified. Besides, γ is the damping coefficient, $\mathbf{F} = \mathbf{\Phi}^T \mathbf{f}$ is the modal participation factor of the load $\mathbf{f}$, with $\mathbf{\Phi}$ the tuned mode shapes of the system, $\mathbf{\Lambda_0}$ is the generalized stiffness matrix of the tuned structure imported from the numerical model. The experimental measurements give the actual eigenfrequencies of the system ω, and $\mathbf{p} = \mathbf{\Phi}_{exp}^{-1}\mathbf{x}_{exp}$ are the modal coordinates computed using the measured physical displacement $\mathbf{x}_{exp}$, and the matrix of tuned mode shapes $\mathbf{\Phi}_{exp}$. Furthermore, $\mathbf{Q}_n$ is the participation factor defined as

$$\mathbf{Q}_n = \mathbf{\Lambda}^{CB^{-1}} \mathbf{\Phi}^{CB^T}\, \mathbf{K}^{CB} \Phi_n, \tag{2}$$

where Λ^{CB} is a diagonal matrix containing the squared eigenfrequencies of a clamped beam, n the number of blades of the blisk, $\mathbf{\Phi^{CB}}$ the cantilever blade modes, and $\mathbf{K}^{CB}$ the cantilever blade stiffness matrix.

The ICMM relies on two major hypothesis: the mistuning in the blisk should be small and the blisk frequency response must have regions with high modal density. These assumptions are realistic considering industrial blisks since the manufacturing tolerance is of the order of few micrometers. Besides, considering industrial blisks, the first family and the second family of mode shapes are well separated from other modes and the corresponding frequency ranges are small.

3.2 Experimental measurements

The preparation of the experimental and numerical inputs for the ICMM method is the most time-consuming part of the process. The developed test rig allows to reduce the complexity of the measurements and automates the process. The experimental test rig, illustrated in Fig. 2(a), uses an electrodynamic shaker, a Laser Doppler Vibrometer and a robotic arm. Each component presents major benefits for the mistuning identification.

Compared to the procedure of Holland *et al.* [12] which used a nodal diameter excitation, a shaker excitation is considered in this paper. The electrodynamic shaker has the advantage to excite the whole structure uniformly compared to the blade to blade speaker excitation for example, which may add external mistuning due to the variation in the separated excitation. The addition of a piezoelectric shaker above the electrodynamic one offers the opportunity to extend the frequency range up to 20 kilohertz. The blisk is fixed to the shaker head through an interface plate, as seen in Fig. 2(a).

The Laser Doppler Vibrometer (LDV) performs contact-less measurements of the velocity. As a result, the dynamic behavior of the structure is not affected by the measurements. The high-frequency stability of the laser signal ensures a sensitivity in the picometer range [14]. The infrared laser technology integrated in the LDV allows avoiding the requirement of reflective patches. This prevents introducing additional mistuning in the actual blisk studied.

The robotic arm serves to automate the tedious work of manually moving the LDV above each blade during the experimental modal analysis. Furthermore, manual positioning is error-prone. Therefore, being able to program the control of the six joints robot to achieve specific positions and orientations of the laser increases test efficiency and accuracy. The robotic arm is fixed upside down to a gantry and the first joint is aligned with the shaker axis to simplify the programming and reduce the positioning absolute errors when rotating around the blisk. The measurements are fully automated all around the blades. The robotic programming allows performing 3D measurements using only one unidirectional LDV with few human actions, which is unfeasible manually within acceptable tolerances.

(a) Experimental test rig

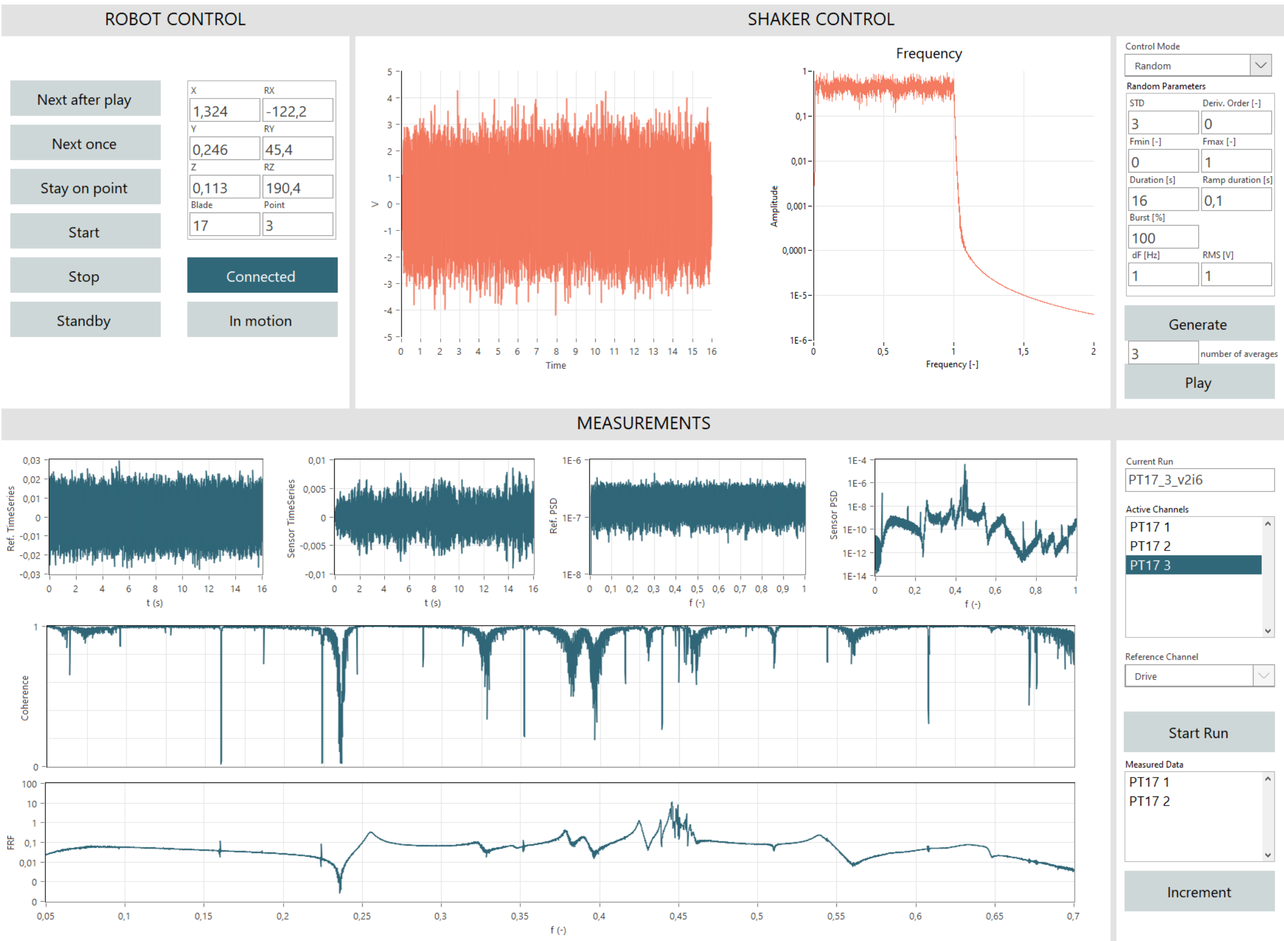

(b) DACS interface

Figure 2: Experimental measurements tools

A Data Acquisition and Control System (DACS) is designed using *LabVIEW* software for the purpose of this study. The DACS interacts with the robotic arm to move the LDV at the desired position, excites the shaker and takes the measurements with the LDV. All the process is automated and requires no human intervention, which increases the efficiency. The DACS user interface is illustrated in Fig. 2(b).

4 Application to an industrial blisk

The industrial blisk investigated is an industrial one-piece bladed structure of 36 sectors made of titanium alloys. For confidential reasons, the blisk eigenfrequencies and the main geometrical characteristics are not made public and the results are all normalized.

The finite element model of the tuned structure is constructed using the *Siemens NX* software and the analysis (modal and Craig-Bampton reduction) are performed using the *Samcef* solver. The model is simplified in order to reduce the computation time. A shell model of the blade is considered in order to converge in frequencies and the numerical solution takes benefit of the cyclic symmetry assumption applicable to the tuned model. More details about this method are given by Madden *et al.* [6]. The structure is clamped at its basis to reproduced the boundary conditions considered when the blisk is fixed to the shaker.

The ICMM method is applied considering only the first bending mode of the clamped blade ($r = 1$) and the first bending mode family of the blisk. Adding modes to the methodology will be the subject of a future study. The first torsion mode family is in the frequency range of the electrodynamic shaker used. The addition of the piezoelectric shaker is useful to excite higher bending and torsion mode families. The mistuning identifier with the proposed methodology is validated considering two approaches. The improvement of the input parameters is then studied to assess the impact on the muistuning pattern identified.

4.1 Validation of the proposed methodology

For the validation of the proposed mistuning identification procedure, only one measurement point per blade along the vertical direction is considered. The experimental modes used in the mistuning identification procedure are selected considering the degree of complexity of the modes. For that purpose, the Modal Phase Collinearity (MPC) and the Mean Phase Deviation (MPD) indicators are computed, the mathematical expression of theses indicators are given by Heylen *et al.* [15]. The experimental mode shapes with a MPC larger than 90% and a MPD lower than $20\,\mathrm{deg}$ are retained to compute the mistuning pattern.

Validation using blade detuning

The mistuning patterns λ_n^E identified with the proposed methodology for the actual blisk are illustrated in Fig. 3 (—○—). The results are validated using the detuning blade methodology [2]. This method allows isolating the vibration of one blade by shifting down the other ones using detuning masses on these ones. The mistuning patterns are linked to the inherent blade mistuning corresponding to the variation in the single blade eigenfrequencies. The blade frequency mistuning patterns δ_n^ω are thus defined as

$$\delta_n^\omega = \frac{\omega_n - \omega_{\mathrm{ref}}}{\omega_{\mathrm{ref}}}, \tag{3}$$

where ω_n is the eigenfrequency of the isolated blade n, and ω_{ref} is defined as the mean of all the single blades eigenfrequencies. The stiffness mistuning pattern δ_n^E is modeled as a perturbation of the individual blade elastic modulus E_n in the ICMM methodology, and is defined as

$$\delta_n^E = \frac{E_n - E}{E}, \tag{4}$$

where E is the reference Young's modulus of the structure, and E_n the deviation of the nominal Young modulus of blade n. Zhou *et al.* [2] have proposed a relation between the blade-alone frequencies and its elastic modulus considering

$$\omega \propto \sqrt{E}. \tag{5}$$

Combining Eq.3, Eq.4 and Eq.5 allows writing

$$\delta_n^E = 2\delta_n^\omega + (\delta_n^\omega)^2 . \tag{6}$$

The mistuning patterns δ_n^E identified with the blade detuning method are shown in Fig. 3 (—□—). The mistuning identification methodology proposed and the blade detuning method shows similar trends. The main peaks are located at the same blades, and their amplitudes are very close to each other. Nonetheless, the isolated frequencies considered in the blade detuning test represent not purely the 'blade-alone' modal frequencies, but blade-dominant modal frequencies. The inter-blade coupling is not completely eliminated by using detuning masses [2], which explains partly the discrepancies in the identified mistuning patterns with both approaches.

Figure 3: Mistuning patterns identified with the proposed methodology (—○—) and with the detuning blade method (—□—)

The studied blisk has been equipped with four strain gauges placed on blades as part of an operating test for the manufacturer. Some damages have results from this test and the blade 4,14,26 and 36 illustrated in Fig.4 have been impacted. These blades clearly stand out in Fig.3.

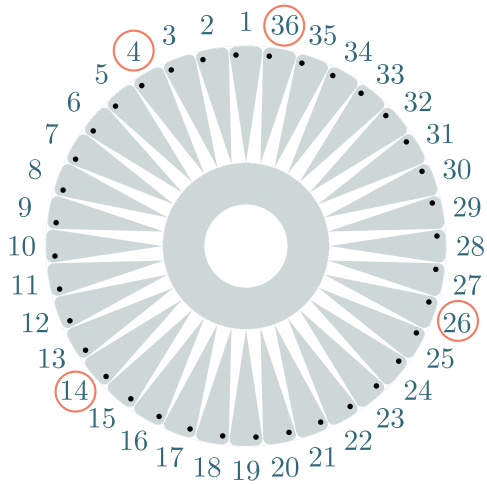

Figure 4: Blades instrumented with strain gauges (○)

Validation using additional masses

The proposed mistuning identification methodology is validated using additional masses to force a known mistuning. Two additional beeswax masses are sticked to the blades 14 and 36, as illustrated in Fig.5(a). The weights and positions of the added masses are summarized in Fig. 5(b).

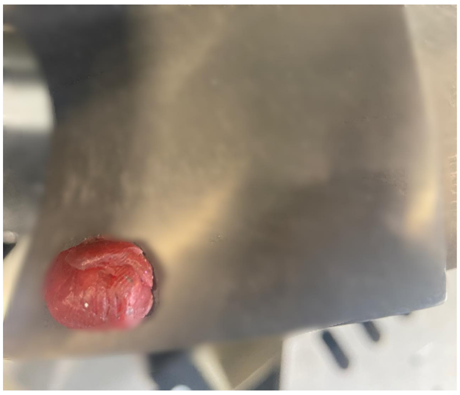

(a) Additional mass

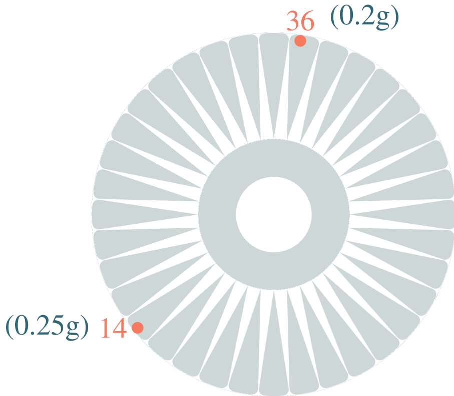

(b) Blades with additional masses (●)

Figure 5: Detuning blade methodology

The mistuning patterns identified with the proposed methodology are illustrated in Fig. 6 (—o—). The mistuning values of the blades where the masses are added are lower than the other ones. The addition of mass decreases their clamped blade eigenfrequencies [11]. The results allow the identification of the disrupted blades and thus validate the proposed mistuning identification methodology.

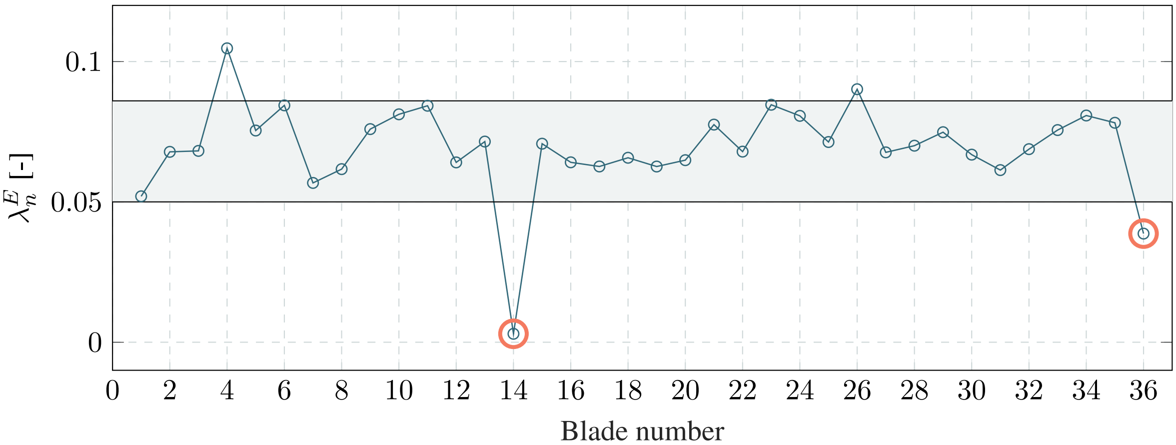

Figure 6: Mistuning patterns identified (—o—) with additional masses (○)

4.2 Improvement of the experimental input data

The accuracy of the mistuning identification technique relies on the quality of the experimental measurements, thus the quantity and the locations of the considered measurement points. If the set of measurement points is too small or unidirectional, the modes could be badly represented and spatial aliasing could occur. This is particularly true for blisks which have eingenfrequencies close to each other, and blades deformations which are not unidirectional. Additional time to get a large number of measurements is not a major concern in the proposed methodology since the measurement process require no human intervention.

A 3D experimental modal analysis can be used in the ICMM methodology. Measurements in the three directions of the plane are nonetheless not always achievable with the LDV considering the twisting of the blisks blades. The feasibility of reconstructing 3D measurements by measuring oblique FRFs is studied.

3D measurement principle and optimal orientation

The unidirectional measurement of the LDV is its major drawback since a precise modal analysis test campaign for industrial blisks requires the identification of modes in the 3 directions of the space. The use of three LDVs is a possibility to achieve such 3D vibration measurements but the method is costly and it is not always feasible to attach 3 LDVs on a robotic arm. has a notable disadvantage considering its high cost. Therefore, the methodology of Khalil *et al.* [16] using one LDV to measure the vibrations in three different directions to reconstruct the 3D vibration components is used. As suggested by K. Shin *et al.* [17], a Frequency Response Function (FRF) is actually nothing more than a vector quantity: a response amplitude in a given direction. The oblique Frequency Response Function $\mathbf{H}_{\text{ob}}$ can be expressed as a linear combination of FRFs measured in x, y and z directions $\mathbf{H}_{\text{x}}, \mathbf{H}_{\text{y}}, \mathbf{H}_{\text{z}}$ at the same point [17], such as

$$\boldsymbol{H}_{\text{ob}} = \cos\alpha\,(\boldsymbol{H}_{\text{x}}) + \cos\beta\,(\boldsymbol{H}_{\text{y}}) + \cos\gamma\,(\boldsymbol{H}_{\text{z}}) = \mathbf{P}\boldsymbol{H}, \tag{7}$$

where α, β and γ fix the orientations of the LDV. The angles are defined between the global coordinates system x, y and z and the coordinates system x', y' and z' fixed by the LDV, as illustrated in Fig.7.

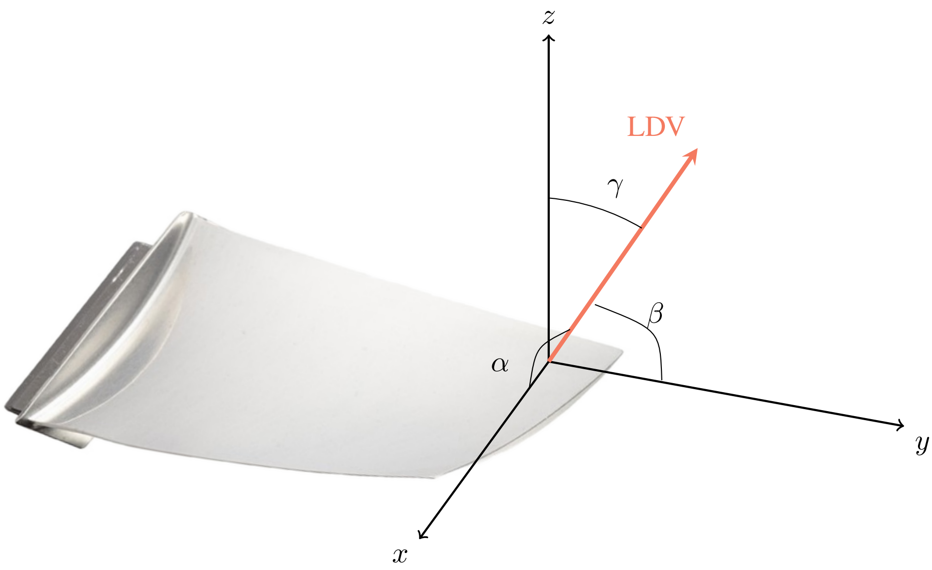

Figure 7: Measurements orientations and projections [18]

The twisting of the blades make impossible measurements in horizontal directions for the considered blisk. Oblique FRFs are thus measured to reconstruct FRFs in the global axes x, y and z. Considering the system of three unknowns $\boldsymbol{H}_{\text{x}}, \boldsymbol{H}_{\text{y}}$ and $\boldsymbol{H}_{\text{z}}$, a minimum of $N = 3$ oblique measurements is required to compute the FRFs in the x, y and z directions. The FRFs in the global coordinates are computed by multiplying Eq.7 by the pseudo inverse of $\mathbf{P}$ as

$$\begin{pmatrix} \boldsymbol{H}_{\text{x}} \\ \boldsymbol{H}_{\text{y}} \\ \boldsymbol{H}_{\text{z}} \end{pmatrix} = \begin{pmatrix} \cos\alpha_1 & \cos\beta_1 & \cos\gamma_1 \\ \cos\alpha_2 & \cos\beta_2 & \cos\gamma_2 \\ \cos\alpha_{..} & \cos\beta_{..} & \cos\gamma_{..} \\ \cos\alpha_i & \cos\beta_n & \cos\gamma_n \end{pmatrix}^{-1} \begin{pmatrix} \boldsymbol{H}_{\text{ob1}} \\ \boldsymbol{H}_{\text{ob2}} \\ \boldsymbol{H}_{..} \\ \boldsymbol{H}_{\text{obn}} \end{pmatrix}, \tag{8}$$

where n is the number of oblique measurements performed. The accuracy of the oblique FRFs measured and the noise of the LDV depend on the measurements angles considered [16]. An analysis of the reconstructed

FRFs accuracy depending on the measurements angles is conducted to choose the best measurement set up for the mistuning identification.

Measurements are performed by considering various half-apex angles Φ for the oblique FRFs measurements, as illustrated in Fig. 8. Four different cone openings, summarized in Table. 1, are considered and compared. For each cone, five orientations of the LDV are considered, as illustrated in Fig. 8 (.....). Three to five oblique directions per cone angle are used to reconstruct FRFs in the global axis. The results are compared by computing the R-Squared between a FRF of reference $\hat{\boldsymbol{H}}_z$ measured in the z direction and the FRF reconstructed using oblique measurements. The R-Squared statistic is defined as

$$R^2 = 1 - \frac{\sum_{\omega=1}^{N_\omega} \left(|\boldsymbol{H}_z(\omega)| - \left| \hat{\boldsymbol{H}}_z(\omega) \right| \right)^2}{\sum_{\omega=1}^{N_\omega} \left(|\boldsymbol{H}_z(\omega)| - \bar{\boldsymbol{H}}_{\mathrm{z}} \right)^2}, \tag{9}$$

where $\bar{\boldsymbol{H}}_{\mathrm{z}}$ is the mean of the reconstructed FRF $\boldsymbol{H}_{\mathrm{z}}(\omega)$ on the frequency range of interest $[\omega_1, \omega_2]$ of size N_ω.

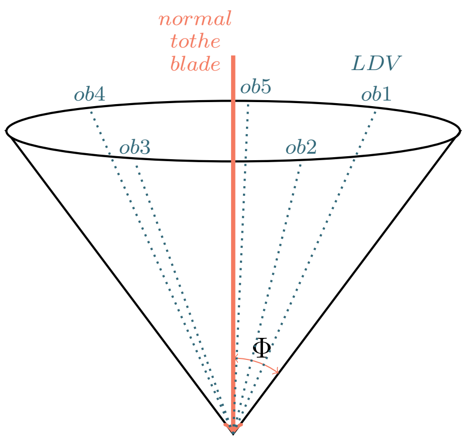

Figure 8: Measurements orientations around the normal

Table 1: Half-apex angles

Case n°	1	2	3	4
Φ [deg]	10	20	30	45

The R-Square indicators for the considered half-apex angles with three to five oblique measurements directions for each cone are illustrated in Fig. 9. Increasing the number of measurements around the cone statistically improve the accuracy of the reconstructed FRFs. Since the FRF in z direction is considered in Fig.9, this conclusion is not significantly illustrated but increasing the number of orientations improves the results in the horizontal directions. The cone angle also improve the results but to some extend because the noise of the LDV measurement is increased when the laser differs too much from the normal to the surface considered. Indeed, the measured velocity is lower as the angle is increased, as illustrated in Fig. 10. This is due to the fact that the blade displacement is mainly in the direction of the normal for the considered blisk and the horizontal displacements components are relatively small compared to the vertical component. Choosing $\Phi = 20$ as cone angles and measuring five FRFs in various directions on the cone is a good compromise between time, accuracy and signal-to-noise ratio in the measurements. The coherence is quite similar between all the measurements as seen in Fig. 10. The reconstructed FRFs in the global axis considering an angle $\Phi = 20$ deg and five orientations are illustrated in Fig. 11.

The results show that the best measurement orientations are case-specific. The twisting and the length of the blades is different for most of the produced industrial blisks. A 3D modal analysis of one sector is particularly valuable as a first step to determine the main deformation orientations. The improvement in the mistuning pattern identified will be the aim of a further work.

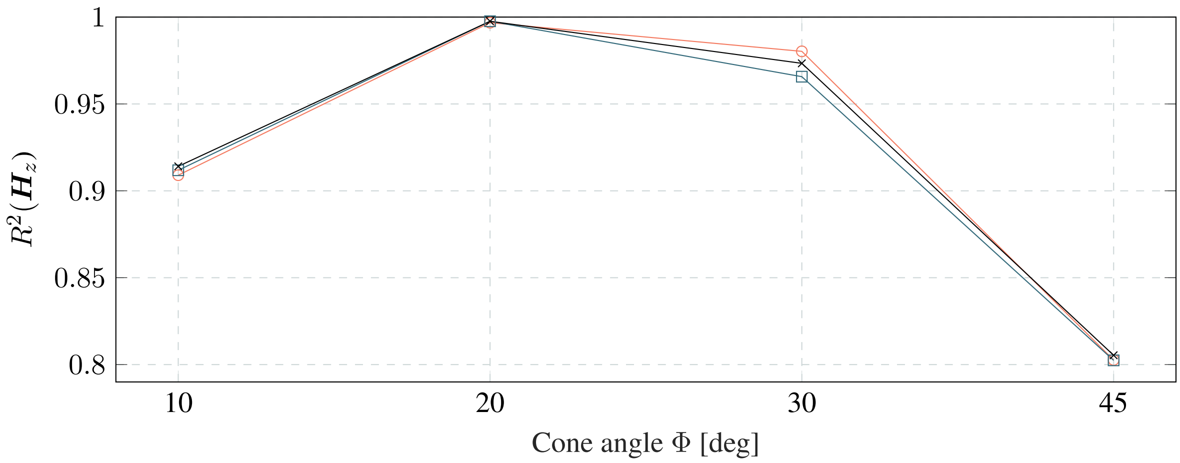

Figure 9: R-Squared statistics for the reconstructed FRFs $\boldsymbol{H}_z$ for different number of measurements: 5 directions (—○—), 4 directions (—□—) and 3 directions (—×—)

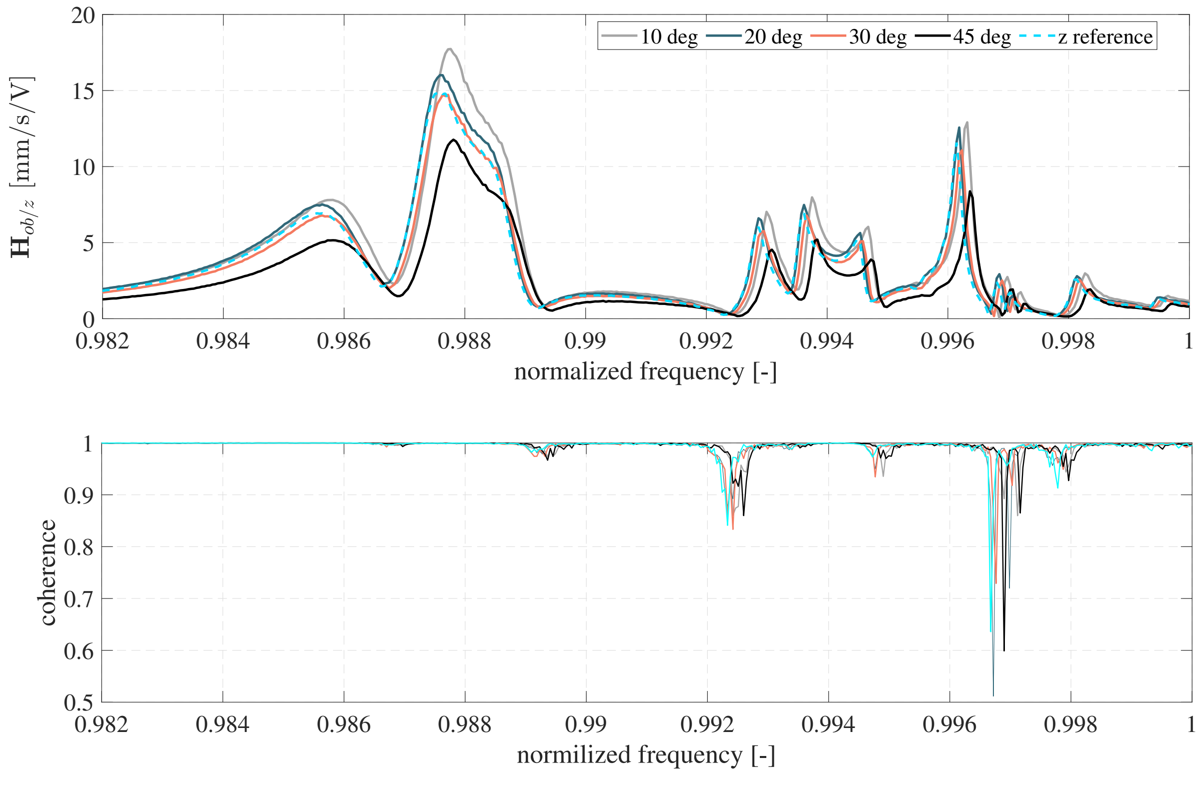

Figure 10: FRFs and coherence measured in oblique directions for various Φ and in z direction

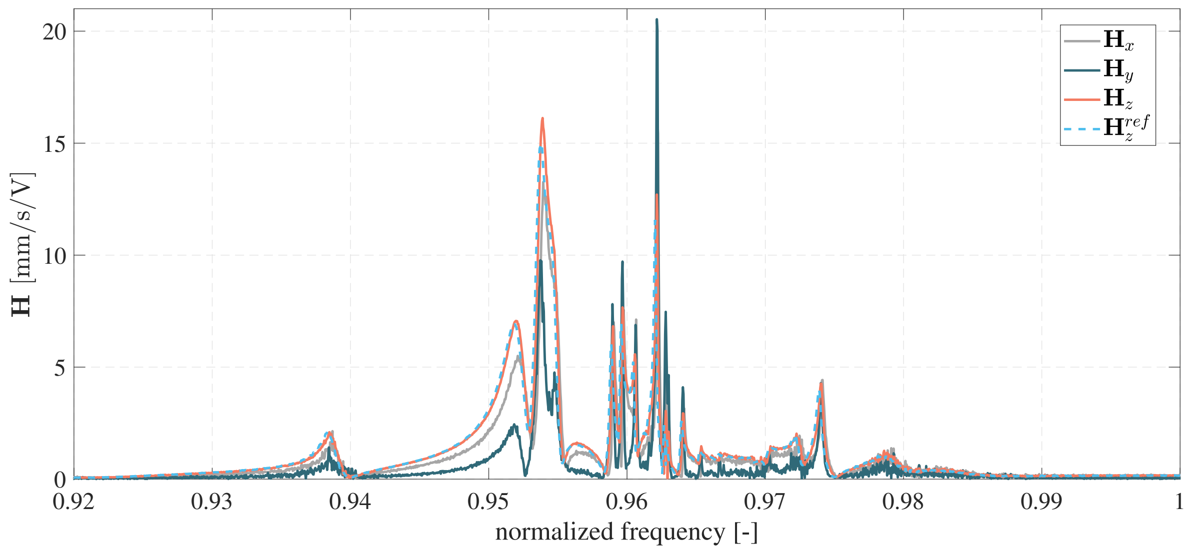

Figure 11: Reference FRF in z-direction, and FRFs reconstructed in x, y and z directions considering oblique FRFs with a cone angle $\Phi = 20$

Number of measurements points

Now that a procedure to perform 3D measurement has been defined, multiple measurement points are considered and the improvement of the identified mistuning is analysed. The best measurement points can be selected by considering the effective independence distribution vector EIDV method proposed by Penny *et al.* [19]. They demonstrate that each harmonic in a considered mode family has a specific optimal set of measurement points. Overall, their approach shows that choosing the tip of the Leading Edges (LE) when measuring first bending modes shape is a good choice. On the basis of the study of Beck *et al.* [20], selecting measurement points close to the defects inducing the mistuning gives the best results. As in the current application, some blades are damaged at the Trailing edges (TE), this is also a good location to measure the responses in the proposed mistuning identification methodology. Measurement points are taken at both the TE and LE of the blades, as illustrated in Fig.12.

Figure 12: Measurement points [18]

The identified mistuning patterns considering only one measurement point at the TE and at the LE of each blade separately, and considering both points together are illustrated in Fig. 13. Increasing the number of measurement points per blade improves the quality of the modal analysis. The obtained mistuning pattern considering both points together is therefore considered as a reference to compare the results obtained with only one measurement point. The correlation coefficients computed are summarized in Table 2. The difference is relatively small since the first bending mode family is considered. Increasing the number of measurement points would have a greater interest considering torsion modes or other higher frequency mode shapes.

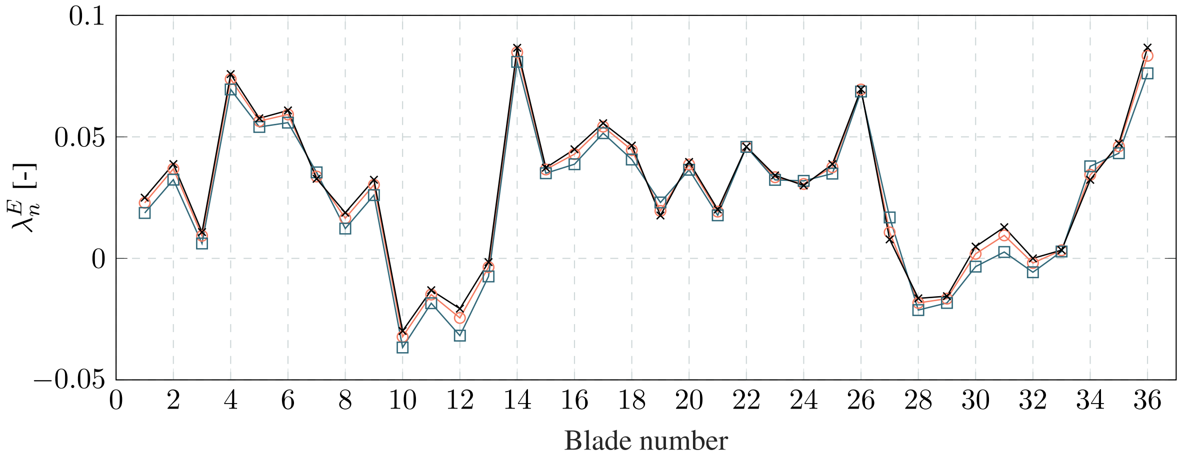

Figure 13: Mistuning identified using the TE (—○—) and LE (—□—) measurement points and the LE and TE points both together (—×—)

Table 2: Correlation coefficients between one or two measurement points at the TE and LE

Measurement point	LE	TE
Correlation coefficient	0.988	0.997

5 Conclusions

An autonomous experimental test rig for the identification of blisks mistuning is proposed and developed. The set-up is composed of an electrodynamic shaker, which provides excitation over the frequency range of the first bending and torsion modes of most industrial blisks. The coupling of a piezoelectric shaker is feasible to extend the frequency range for further analyses to consider higher frequency modes of the blisk. The LDV used to carry out the measurements is positioned thanks to a robotic arm. The test rig provides the possibility to easily vary the measurement direction of the LDV to perform 3D measurements. The robotic arm enables the user to accurately chose the measurement points, to automatically scan all the blisk blades and to preform 3D measurements.

The validation procedure shows good results. The mistuning patterns identified with the proposed test rig and the ICMM methodology are similar to the patterns obtained using the detuning blade methodology. Besides, adding masses to force known mistuning patterns has also shown satisfying identification of the mistuning with the proposed methodology.

The precise positioning of the robotic arm and the use of one LDV have made possible 3D vibration measurements. Five oblique measurements with various angles to the normal to the blade are considered. The FRFs in the global axis of the blisk are reconstructed to determine the directions giving the most accurate FRFs in the three main directions. Considering an angle of 20 degrees is a good compromise between the accuracy of the reconstructed FRFs and the measurement signal-to-noise ratio for the considered blisk. The best direction is nonetheless dependent on the studied structure according to the blade twisting and length. A 3D modal analysis of one sector of the blisk of interest is valuable to determine the best orientation.

The analysis of the number of measurement points per blade for the experimental modal analysis reaches the same conclusion. The choice must be adapted considering the mode shape of interest and thus the geometry of the blade itself. Overall, the mistuning pattern identified with multiple measurement point on the same blade is not significantly improved but if torsion modes or higher bending modes are considered, measuring only one point per blade will be a limiting factor for the modal analysis. Combining multiple points per blades and 3D measurements to determine the mistuning patterns is the subject of a forthcoming study. In particular, the usefulness of the tools proposed for higher frequency modes will be investigated.

Acknowledgements

The present work is carried out in the framework of the Coopilot ”VIBE” project funded by Wallonia DG06 and FEDER under contract N°1910246.

We would like to thank Safran Aero Boosters who has made available a blisk for the purpose of the feasibility demonstration.

References

[1] D. Tudor, “Innovative measuring solutions enhance blisk production - PES Media,” 01 2021. [Online]. Available: https://www.pesmedia.com/renishaw-blisk-metrology-27012021/

[2] B. Zhou, J. Zhao, and T. M. Berruti, “Exploration of blade detuning tests for mistuning identification of blisks,” *Mechanical Systems and Signal Processing*, vol. 175, p. 109118, 2022. [Online]. Available: https://www.sciencedirect.com/science/article/pii/S0888327022002837

[3] C. Pierre, “Mode localization and eigenvalue loci veering phenomena in disordered structures,” *Journal of Sound and Vibration*, vol. 126, no. 3, pp. 485–502, 1988.

[4] R. Bladh, C. Pierre, M. Castanier, and M. Kruse, “Dynamic response predictions for a mistuned industrial turbomachinery rotor using reduced-order modeling,” *Journal of Engineering for Gas Turbines and Power*, vol. 124, no. 2, p. 311, 2002.

[5] J. A. Judge, C. Pierre, and S. L. Ceccio, “Experimental Mistuning Identification in Bladed Disks Using a Component-Mode-Based Reduced-Order Model,” *AIAA Journal*, vol. 47, no. 5, pp. 1277–1287, 2009.

[6] A. C. Madden, M. P. Castanier, and B. I. Epureanu, “Reduced-Order Model Construction Procedure for Robust Mistuning Identification of Blisks,” *AIAA Journal*, vol. 46, no. 11, pp. 2890–2898, 2008.

[7] P. Vargiu, C. Firrone, S. Zucca, and M. Gola, “A reduced order model based on sector mistuning for the dynamic analysis of mistuned bladed disks,” *International Journal of Mechanical Sciences*, vol. 53, no. 8, pp. 639–646, 2011. [Online]. Available: https://www.sciencedirect.com/science/article/pii/S0020740311000993

[8] M. P. Castanier, G. O´ttarsson, and C. Pierre, “A Reduced Order Modeling Technique for Mistuned Bladed Disks,” *Journal of Vibration and Acoustics*, vol. 119, no. 3, pp. 439–447, 07 1997. [Online]. Available: https://doi.org/10.1115/1.2889743

[9] S.-H. Lim, R. Bladh, M. P. Castanier, and C. Pierre, “Compact, Generalized Component Mode Mistuning Representation for Modeling Bladed Disk Vibration,” *AIAA Journal*, vol. 45, no. 9, pp. 2285–2298, 2007.

[10] F. Nyssen and J.-C. Golinval, “Identification of mistuning and model updating of an academic blisk based on geometry and vibration measurements,” *Mechanical Systems and Signal Processing*, vol. 68, pp. 252–264, 2016.

[11] F. Nyssen, B. Epureanu, and J.-C. Golinval, "Experimental modal identification of mistuning in an academic two-stage drum," *Mechanical Systems and Signal Processing*, vol. 88, pp. 428–444, 2017.

[12] D. E. Holland, M. P. Castanier, S. L. Ceccio, B. I. Epureanu, and S. Filippi, "Testing and Calibration Procedures for Mistuning Identification and Traveling Wave Excitation of Blisks," *Journal of Engineering for Gas Turbines and Power*, vol. 132, no. 4, 2010.

[13] F. Pichot, D. Laxalde, J.-J. Sinou, F. Thouverez, and J.-P. Lombard, "Mistuning identification for industrial blisks based on the best achievable eigenvector," *Computers & Structures*, vol. 84, no. 29-30, pp. 2033–2049, 2006.

[14] C. Rembe and R. Kowarsch, "High-resolution laser-vibrometer microscopy," 06 2017.

[15] W. Heylen, S. Lammens, and P. Sas, *Modal analysis theory and testing.*, revised ed. Leuven,Belgium: Department of Mechanical Engineering, Katholieke Universiteit Leuven, 1997.

[16] H. Khalil, D. Kim, J. Nam, and K. Park, "Accuracy and noise analyses of 3D vibration measurements using laser Doppler vibrometer," *Measurement*, vol. 94, pp. 883–892, 2016.

[17] S. Y. Khoo, Y. C. Lian, Z. C. Ong, Z. Ismail, and S. Noroozi, "Feasibility study of performing experimental modal analysis with oblique impact testing using various oblique impact directions," *Alexandria Engineering Journal*, vol. 59, no. 1, pp. 457–473, 2020.

[18] "Engine blade - OTEC Präzisionsfinish GmbH," 2022. [Online]. Available: https://www.otec.de/en/news/otec-news/2018/engine-blade/

[19] J. E. T. Penny, M. I. Friswell, and S. D. Garvey, "Automatic choice of measurement locations for dynamic testing," *AIAA Journal*, vol. 32, no. 2, pp. 407–414, 1994.

[20] J. Beck, A. Kaszynski, J. Brown, D. Gillaugh, and O. Scott-Emuakpor, "Selection of dynamic testing measurement locations for integrally bladed disks," 06 2018, p. V07CT35A037.